

Article

# An Approach to the Paleoceanographic Characteristics of the Sea-Surface at the Western Mediterranean (Balearic Area) during the Pliocene and Gelasian

Francisco Serrano

Departamento de Ecología y Geología, Universidad de Málaga, Campus de Teatinos s/n, 29071 Málaga, Spain; F.Serrano@uma.es

Received: 24 June 2020; Accepted: 4 August 2020; Published: 7 August 2020



**Abstract:** From the study of the planktonic foraminifer assemblages of the sediments of the Ocean Drilling Program (ODP)-Site 975 (Balearic), sea-surface temperature, seasonality and salinity for the Pliocene and Gelasian of the Western Mediterranean were estimated. The estimates were carried out by the modern analog technique (MAT) using PaleoUma, a calibration dataset of 735 North-Atlantic and Mediterranean core-tops. In order to compare Pliocene–Gelasian and present-day analog assemblages, the necessary reduction of the taxonomic variables leads to statistically insignificant increases in estimation error, assessed on the calibration dataset itself. In addition, the correlation with  $\delta^{18}\text{O}$  results as an independent proxy, supports the use of MAT in order to establish the dominant paleoceanographic frameworks during the Pliocene and Gelasian. The SST curve shows an increase trend of the average value since the Early Zanclean ( $19.7 \pm 1.8$  °C) to the Late Piacenzian ( $20.9 \pm 1.7$  °C) and a decrease until the Late Gelasian ( $18.1 \pm 1.4$  °C). The seasonality offers permanently lower estimates than the current value (9.8 °C), reaching the closest values during the Late Gelasian ( $8.6 \pm 0.8$  °C). The salinity estimates are overall slightly lower during the Zanclean ( $36.7\text{‰} \pm 0.5\text{‰}$ ) than today (37.3‰), whereas they reach up to more than 38.5‰, in the Early Piacenzian. The paleoceanographic frameworks deduced from the combination of the paleoceanographic parameters suggest that the current water-deficit regime in the Mediterranean was clearly predominant throughout the Pliocene and Gelasian. However, since the Piacenzian this regime alternates with stages of water surplus, which are especially frequent in the late Piacenzian. By the middle of the Early Gelasian the regime becomes more predominantly in deficit again.

**Keywords:** paleoceanography; Pliocene; Gelasian; western Mediterranean; planktonic foraminifera; modern analog technique (MAT)

## 1. Introduction

In the present-day, the Mediterranean water-mass is subject to a thermohaline circulation due to, in origin, the hydric deficit of the inputs by direct rain and fluvial supplies vs. to evaporation losses. The inflow of cool Atlantic surface water coming from northern latitudes compensates the deficit. Nevertheless, the volume of the Atlantic water entering the Mediterranean through the Straits of Gibraltar is some 20 times greater to that required to compensate for this deficit [1–3]. This excess results in an outflow of deeper and more saline Mediterranean water towards the Atlantic.

The incoming surface water from the Atlantic, due to the Coriolis effect, flows mainly close to the African coastline reaching partially the Eastern Mediterranean through the Straits of Sicily (Figure 1). The Balearic area is affected by the major cyclonic circulation of the Algeria–Provence basin and subsidiary wind-induced anticyclonic eddies [4,5]. In summer, the Atlantic-in-origin surface water, overheated by insolation, is mixed with the more surface part of the warmer, more saline Levantine

Intermediate water coming from the Eastern Mediterranean, so reaching temperatures more than 23.5 °C. In winter, the predominant northern dry winds from the continent cool the surface water and favored the formation of deep-water in the northern part of the Western Mediterranean, which are incorporated into the cyclonic motion extending as far as the Balearic Islands at temperature below 14 °C. This oceanographic setting explains the high seasonality close to 10 °C of the sea surface at the Balearic area.



**Figure 1.** Predominant surface currents in the Western Mediterranean Sea and location of the Ocean Drilling Program (ODP)-site 975. LIW: Levantine intermediate water. Geographic basis from image Landsat, Google Earth.

The hydric deficit has not been permanent in the Mediterranean. The noticed most extreme case occurred at the end of the Messinian, characterizing the Lago-Mare event [6], in which the increase in the freshwater contribution led to a surplus in the Mediterranean water budget and the establishing of the a thick brackish surface layer [7–9].

This study attempts an approaching to the knowledge of the oceanographic characteristics of the sea-surface at the Western Mediterranean during the Pliocene and Gelasian. For this, values of temperature, seasonality and salinity of the sea-surface are estimated at a high-middle resolution throughout the referred time interval. Considering that the Mediterranean geotectonic and paleogeographic setting has not changed significantly since the beginning of the Pliocene, the variations of the paleoceanographic parameters must be caused by climate change. However, climate changes affecting to the hydric balance can result in different flow patterns, accentuating or lessening the changes of the oceanographic parameters in the Western Mediterranean with respect to the Global Ocean. Consequently, paleoceanographic frameworks consistent with the results of the sea-surface parametric values are proposed.

## 2. Materials

The ODP-Site 975 is located in the Balearic area (Figure 1), to the south of Menorca (38°53.82' N, 4°30.6' E) with a water depth of 2415 m [10]. In this site, Gelasian and Pliocene sediments were drilled between 125.40 and 314.8 mcd (meters composite depth, referred to the different holes drilled at the Site 975) made up by silty and calcareous clay rich in planktonic foraminifera and nannofossils. Color banding and bioturbation are common, especially below 150 mcd [10].

For reaching the proposed aims, 195 samples supplied by the Organization of the Ocean Drilling Program [11] were studied. The samples were picked to intervals close to 1 m and supplied in cylinder

of 2.5-cm diameter. This sampling density involves an average time interval of about 18 ka between consecutive samples and near 450 years represented in each sample.

All studied samples yield abundant, well-preserved planktonic foraminifera and showed no significant traces of reworking or dissolving. This suggests that the taphonomic processes have not significantly altered the composition of the assemblages, at least to affect to the estimates of the oceanographic parameters.

The composition of the planktonic foraminifer assemblages of the ODP-Site 975 samples was quantified by the frequencies of the taxa from more than 300 specimens per sample obtained in the >150  $\mu\text{m}$  fraction (Figure 2 and Supplementary Table S1). The formal names of the taxa are normalized in Table 1.

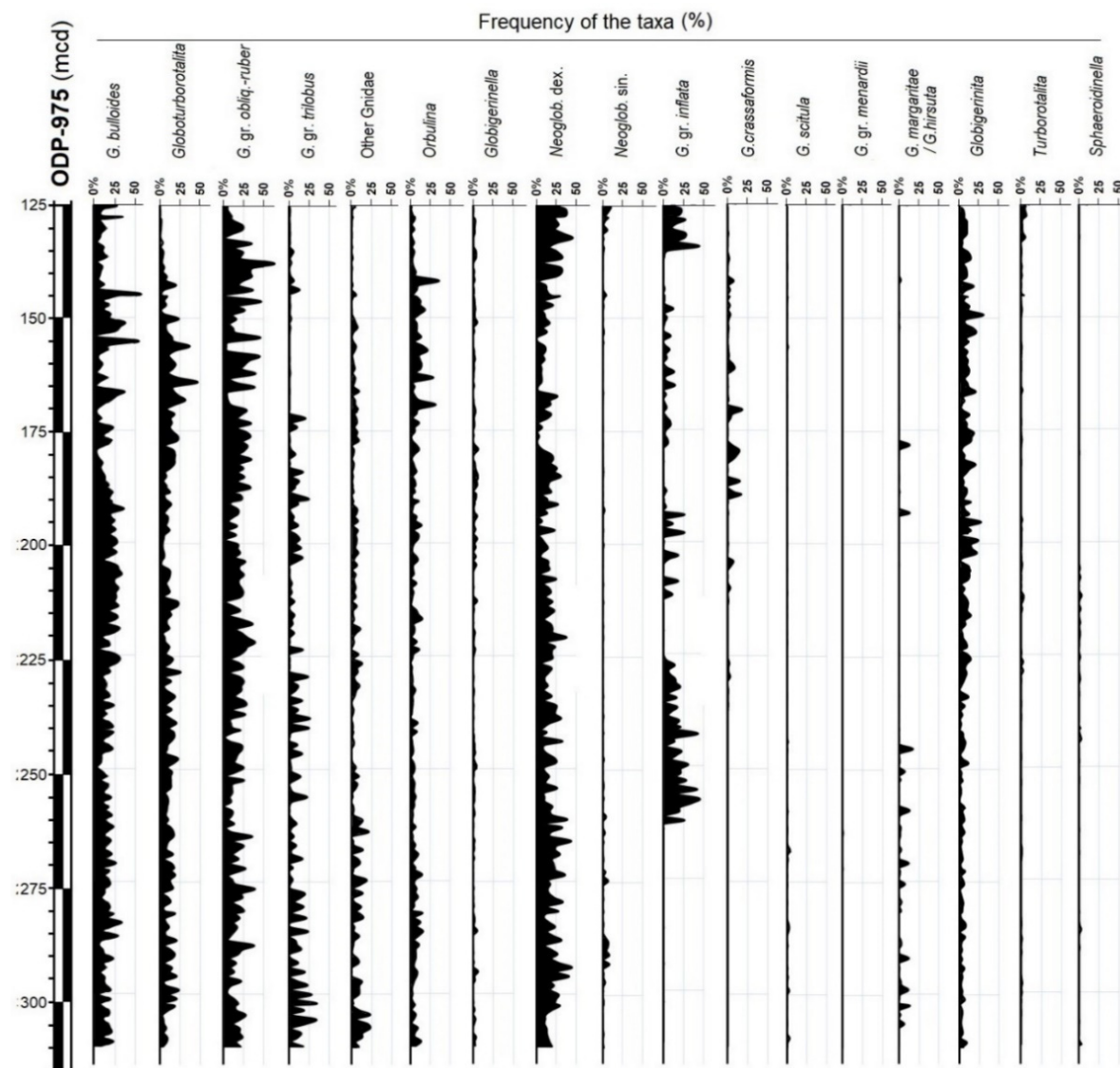


**Figure 2.** Quantitative composition of the assemblages of planktonic foraminifera through Pliocene–Gelasian sediments drilled by the ODP at the site 975. Other Globigerinidae (Gnidae) include: *B. digitata*, *G. calida* and *G. falconensis*; *G. gr. obliq.-ruber* includes: *G. conglobatus*, *G. extremus*, *G. obliquus*, *G. elongatus* and *G. ruber*; *G. gr. trilobus* includes: *G. trilobus* and *G. sacculifer*; *G. gr. inflata* includes: *G. inflata*, *G. bononiensis* and *G. puncticulata*; *Sphaeroidinella* includes *Sphaeroidinellopsis* species.

**Table 1.** Taxonomic appendix with the formal names of the planktonic foraminifera appearing throughout the text.

---

<i>Globigerina bulloides</i> d’Orbigny
<i>Globigerina calida</i> Parker
<i>Globigerina falconensis</i> Blow
<i>Globigerina</i> ( <i>Beella</i> ) <i>digitata</i> (Brady)
<i>Globigerinella</i> ssp. Cushman
<i>Globigerinita</i> ssp. Brönnimann
<i>Globoturborotalita apertura</i> (Cushman)
<i>Globoturborotalita decoraperta</i> Takayanagi & Saito
<i>Globoturborotalita rubescens</i> (Hofker)
<i>Globoturborotalita</i> (“ <i>Globigerinoides</i> ”) <i>bulloideus</i> (Crescenti)
<i>Globoturborotalita</i> (“ <i>Globigerinoides</i> ”) <i>tenellus</i> (Parker)
<i>Globigerinoides conglobatus</i> (Brady)
<i>Globigerinoides extremus</i> Bolli & Bermúdez
<i>Globigerinoides obliquus</i> Bolli
<i>Globigerinoides elongatus</i> (d’Orbigny)
<i>Globigerinoides ruber</i> (d’Orbigny)
<i>Globigerinoides sacculifer</i> (Brady)
<i>Globigerinoides trilobus</i> (Reuss)
<i>Globorotalia bononiensis</i> Dondi
<i>Globorotalia crassaformis</i> Galloway & Wissler
<i>Globorotalia cultrata</i> (d’Orbigny)
<i>Globorotalia hirsuta</i> (d’Orbigny)
<i>Globorotalia inflata</i> (d’Orbigny)
<i>Globorotalia margaritae</i> Bolli & Bermúdez
<i>Globorotalia menardii</i> (Parker, Jones & Brady)
<i>Globorotalia plesiotumida</i> Blow & Banner
<i>Globorotalia puncticulata</i> (Deshayes)
<i>Globorotalia scitula</i> (Brady)
<i>Globorotalia truncatulinoidea</i> (d’Orbigny)
<i>Globorotalia tumida</i> (Brady)
<i>Neogloboquadrina acostaensis</i> (Blow)
<i>Neogloboquadrina atlantica</i> (Berggren)
<i>Neogloboquadrina dutertrei</i> (d’Orbigny)
<i>Neogloboquadrina humerosa</i> (Takayanagi & Saito)
<i>Neogloboquadrina incompta</i> (Cifelli)
<i>Neogloboquadrina pachyderma</i> (Ehrenberg)
<i>Orbulina</i> ssp. d’Orbigny
<i>Pulleniatina</i> ssp. Cushman
<i>Sphaeroidinella</i> ssp. Cushman
<i>Sphaeroidinellopsis</i> ssp. Banner & Blow
<i>Turborotalita</i> ssp. Blow & Banner

---

### 3. Methodology

For estimating the oceanographic parameters, the modern analog technique (MAT) described by [12] is applied, using an ample calibration dataset from North Atlantic-Mediterranean core-tops. Taking in account that the Pliocene and Gelasian planktonic foraminifer assemblages are not analogs to those of the present-day, adaptations are necessary for the comparison.

#### 3.1. The Calibration Dataset

Considering the Mediterranean oceanographic setting, the universe of oceanographic conditions is restricted to the North Atlantic-Mediterranean. In agree with [13] the regionalization of the oceanographic setting avoids noise in the results due to non-discriminant morphologies corresponding to cryptic genetic types with distinct ecologic preferences in other areas. The available CLIMAP database [14] integrates well the conditions represented in the North Atlantic, but semiconfined oceanographic regions such as the Mediterranean or the Gulf of Mexico are poorly represented. A notable option for avoid this gap represents the MARGO calibration data set [15], adding supplementary core-tops to the original CLIMAP database and establishing different regional datasets. Similarly, the PaleoUma calibration

dataset was compiled for the North Atlantic-Mediterranean region in several stages [16–18], from the CLIMAP database, adding core-tops data mainly by [19–22] (available in <http://webpersonal.uma.es/fsl/>). The PaleoUma calibration dataset is made up of 735 samples coming from 576 core-tops throughout the North Atlantic Ocean and 159 core-tops throughout the Mediterranean Sea (Figure 3).

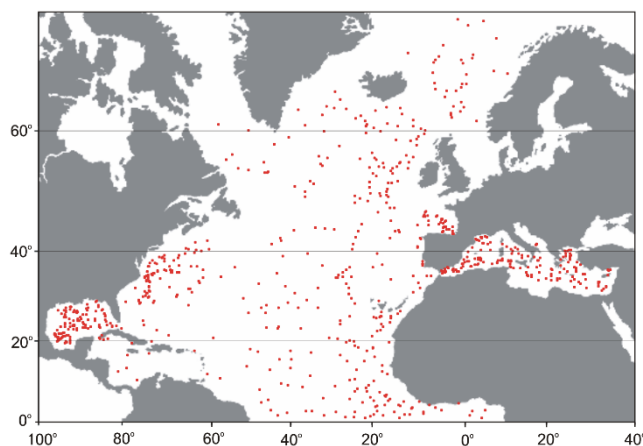


**Figure 3.** Location of the core-tops composing the PaleoUma calibration database.

In the PaleoUma calibration dataset, the planktonic foraminifer assemblages of each core-top sample were quantified, as in CLIMAP database, by the frequencies of 26 taxonomic variables. The sea-surface parameters associated with each core-top sample were: (i) mean annual temperature (SST); (ii) seasonality, considered as the difference between the summer-SST (mean of the warmer three-months) and the winter-SST (mean of the cooler three-months); and (iii) mean annual salinity. The values of these parameters were taken from the NODC-archives of the National Oceanographic Data Center [23] corresponding to the sea surface at 10-m depth in the same geographic coordinates of the core-tops).

The behavior of the PaleoUma calibration database was evaluated [18] by means the comparison between the SST-MAT estimates and the SST-NODC, using a self-evaluation test (the leave-one-out method) and the squared chord distance (SCD) as a measure of similarity. Comparatives performed by different authors [24–28] showed that this technique usually provides more accurate results than other variants of transfer functions developed since [29]. In the present study, using similar methodology, the evaluation is completed for the temperature, seasonality and salinity estimates (Table 2 and Figure 4 Unmodified PaleoUma). The results show that the correlation is very high for the three parameters, with the Pearson coefficient ( $r$ ) ranging between 0.995 for the temperature and 0.950 for the seasonality (in all cases, probability of null hypothesis  $p \ll 0.001$ ). The regression lines adjusted by the least-squares method, practically crosses identical values of MAT and NODC ( $y \approx x$ ) for temperature estimates, while there is a very slight underestimation of MAT for seasonality and salinity towards high values. In all cases, the mean errors resulted lower than 0.6 and similar range of values for the standard deviation. The better results obtained for the temperature estimates were expectable, since in the compilation of PaleoUma database, the core-tops that offered errors more than 2 °C in the SST estimation were removed.

### 3.2. Adjusting Taxonomic Categories in the PaleoUma Calibration Database and the Pliocene–Gelasian ODP-Site 975 Sampling

The list of the taxa of the present-day planktonic foraminifera differs of those recognized in the Gelasian and Pliocene assemblages and, therefore, no direct estimating of paleoceanographic parameters by means of MAT can be made.

**Table 2.** Statistics resulting of the tests of behavior of PaleoUma database adapted to different time-spans of the Gelasian–Pliocene.

Adaptation for Time-Spans	SST (°C)			Seasonality (°C)			Salinity (‰)		
	Mean Error	Mean Abs. Error	Correlation (r)	Mean Error	Mean Abs. Error	Correlation (r)	Mean Error	Mean Abs. Error	Correlation (r)
Unmodified PaleoUma	0.01 ± 0.64	0.47 ± 0.43	0.995	0.06 ± 0.78	0.56 ± 0.55	0.950	−0.01 ± 0.33	0.22 ± 0.25	0.960
Gelasian–Piacenzian	0.00 ± 0.88	0.59 ± 0.66	0.990	0.02 ± 0.98	0.68 ± 0.71	0.919	−0.01 ± 0.40	0.26 ± 0.30	0.942
Upper Zanclean	0.00 ± 0.88	0.59 ± 0.66	0.990	0.02 ± 0.99	0.68 ± 0.72	0.918	−0.01 ± 0.40	0.26 ± 0.30	0.941
Lower Zanclean	0.00 ± 1.03	0.66 ± 0.80	0.986	0.03 ± 1.02	0.71 ± 0.73	0.914	−0.00 ± 0.45	0.29 ± 0.34	0.925

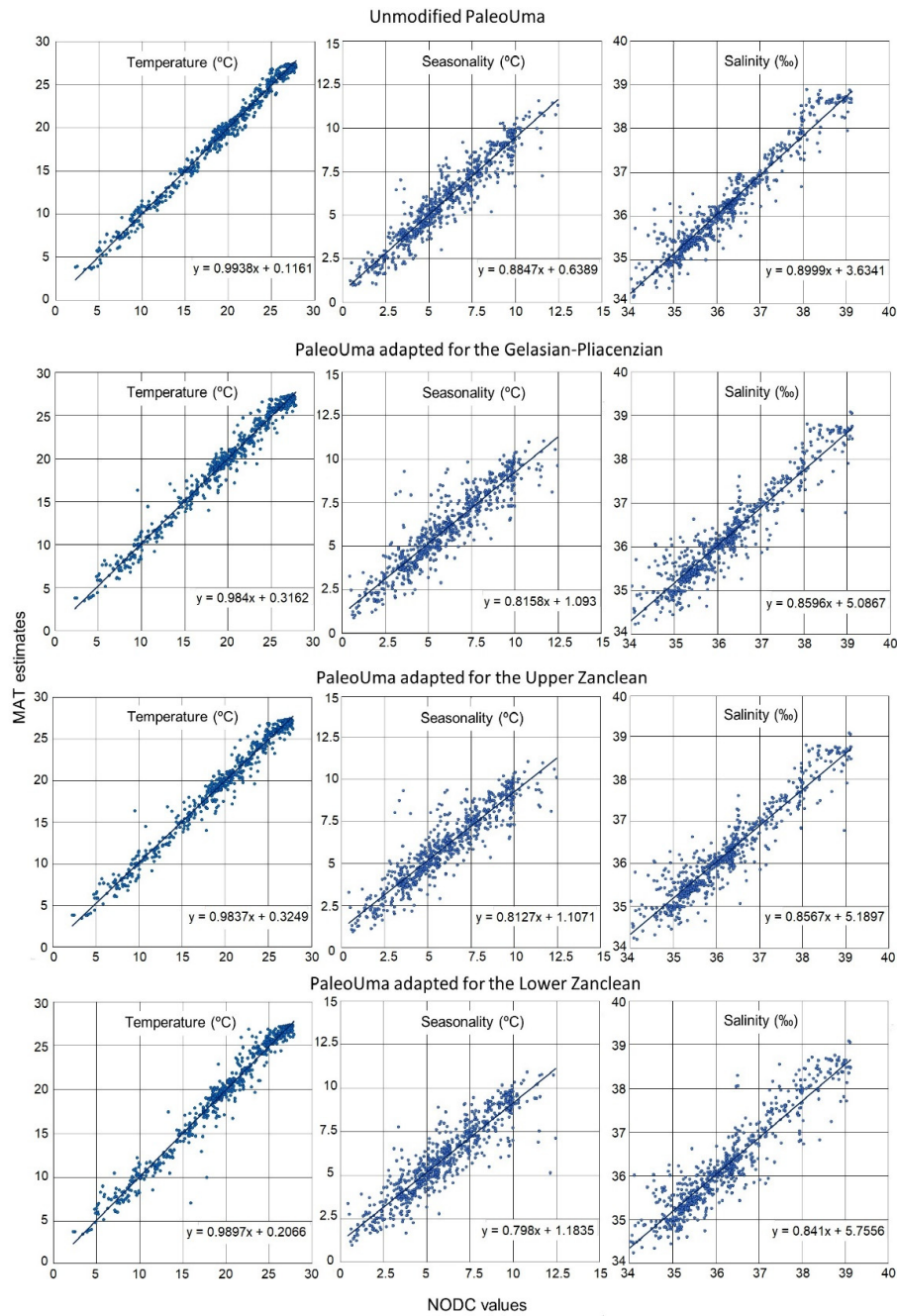


**Figure 4.** Analyzing the behavior of the PaleoUma calibration database by means the leave-one-out method. Comparison between the National Oceanographic Data Center (NOCD) values and modern analog technique (MAT) estimates.

Homogenization of the taxonomic categories removing non-coincident taxa and grouping population-related taxa lead to an approach to analog situations. In general, these modifications should cause increase in the estimation error, which must be evaluated as much as possible.

Regarding the adaptation of the taxonomic categories, a particular case represents *N. pachyderma*, in which seems coexist genetic differences between right and left coiling forms [30–33]. On this basis, [34] proposed to reserve the name *N. pachyderma* for the left-coiling forms only and named *N. incompta* to the right-coiling forms. In addition, [35] concluded that the modern left-coiling forms appeared about 1 Ma ago, thus preventing its use in paleoceanographic reconstructions prior to this age. Moreover, [36] concluded that during the Pliocene-Pleistocene transition (including the Gelasian) two different populations of left-coiling *Neogloboquadrina* could have existed in the Mediterranean with different environmental requirements: one, forms derived from late Miocene-Pliocene (i.e., left-coiling *N. acostaensis*–*N. humerosa*) and another being the ancestor of the modern *N. pachyderma* (left-coiling). In addition, there is uncertainty in the discrimination between *N. dutertrei* and the transitional forms with right-coiling *N. pachyderma* (= *G. incompta*). As a consequence of the above-mentioned, were combined all forms of *Neogloboquadrina* in a single taxonomic category in both, the calibration database and the sampling database.

In addition, *G. truncatulinoides* (right and left forms) and *Pulleniatina* were removed, due to that practically they are not present (just a specimen of *G. truncatulinoides* in an only sample) in the ODP-Site 975 sampling database. Moreover, was necessary remove *G. hirsuta* and, its morphologically close, *G. margaritae*, because both taxa do not coexist, and it cannot be sure to have similar environmental requirements.

On the other hand, as considered in [17], some taxonomic differences between the Pliocene and modern populations represent only increase or reduction of the morphologic variability with frequent transitional forms within the same evolutionary species and, as a consequence, they can be grouped in a simple taxonomic category. In accepting this statement, were grouped:

- *G. ruber* group: *G. ruber*, *G. elongatus*, *G. conglobatus*, *G. obliquus* and *G. extremus*;
- *Globoturborotalita* components: *G. rubescens*, *G. tenellus*, *G. apertura*, *G. decoraperta* and *G. bulloideus*;
- Components of *G. inflata* group: *G. inflata*, *G. bononiensis* and *G. puncticulata*;
- In addition, the warm-water keeled globorotalids, belonging to *G. cultrata* and *G. tumida* groups (including the morphologic variants of each: *G. menardii* and *G. plesiotumida*) were combined, based on that many specimens are difficult to assign unequivocally to one of them.

The preceding modifications lead to a reduction from 26 to 17 taxonomic categories for estimating oceanographic parameters relative to the Gelasian and Piacenzian. The increase of the inaccuracy due to the adaptation of the taxonomic categories with respect to the unmodified PaleoUma is very low. The test of auto-evaluation (Table 2 and Figure 4) mainly shows a slight increase in standard deviation of the mean errors and a statistically insignificant, very slight decrease in the Pearson correlation. The regression lines indicate that MAT tends to overestimate very slightly the results for low seasonality and salinity, while for high values of these parameters, the results are often a bit more underestimated than in the unmodified PaleoUma. This effect was expectable, as the cases with maxima values have their closest analogs with lower values, and vice versa.

Evolutionary changes during Early Pliocene require added modifications. Thus, *G. crassaformis* is not present in older times than the Piacenzian and, as a consequence, this taxonomic category was removed of the calibration dataset for estimates of Zanclean samples. Due to the low weight of this variable in the MAT procedure, the auto-evaluation results on PaleoUma adapted for the Late Zanclean (Table 2, Figure 4) virtually no change from those obtained for Gelasian-Piacenzian.

Moreover, the first representative form of the *G. inflata* group (i.e., *G. puncticulata*) is used as a maker for the beginning of the Late Zanclean. Thus, this taxonomic category was removed of the calibration dataset for estimating Early Zanclean paleoceanographic conditions. Although the *G. inflata* group is usually a major component of the planktonic foraminifer assemblages in warm-temperate environments, the removing as estimation variable lead to a statistically insignificant increase in

estimation error in relation to the results obtained for the time-spans previously analyzed (Table 2, Figure 4).

### 3.3. Estimating Values of the Paleoceanographic Parameters

As in the auto-evaluation tests of the calibration database, paleoceanographic parameters (sea-surface values of temperature, seasonality and salinity) for the Gelasian–Pliocene were estimated by means of MAT using the squared chord distance (SCD) as a measure of similarity. As in [17], for each sample analyzed, the ten closest core-tops of the calibration database are selected and then calculated the mean values of their corresponding oceanographic parameters, weighting inversely respect to their distances from the sample. The SST values correspond to the arithmetic mean of winter and summer sea-surface temperatures (in turn, mean temperature of the three coldest and warmest months, respectively). The seasonality value was calculated as the difference between summer-SST and winter-SST and the salinity values correspond to the annual mean of the monthly salinities.

To explore the correspondence of the results with an independent proxy,  $\delta^{18}\text{O}$  data by [17] obtained of *G. bulloides* specimens from a set of samples of the ODP-975 corresponding to different time intervals (including Lower Calabrian samples) were compared with the SST estimates of the same samples. The comparison shows a noticeably parallel curves if the scale of the  $\delta^{18}\text{O}$  values is reversed (Figure 5) with a significant negative correlation ( $r = -0.629$ ;  $p < 0.001$ ). This correlation must be observed considering the possible response lag between the SST estimates and corresponding  $\delta^{18}\text{O}$  values of the ocean water, as well as the particular oceanographic response of the Mediterranean to climate change, which should lead to a fall in the correlation value.

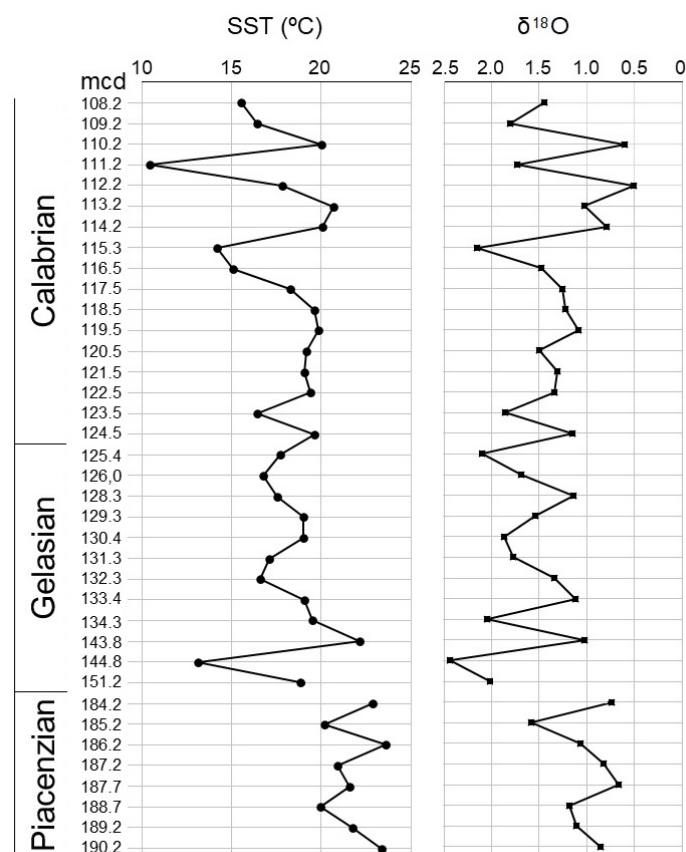


**Figure 5.** SST estimates and  $\delta^{18}\text{O}$  values for Upper Pliocene–Lower Pleistocene samples from the ODP-site 975.

#### 4. Biostratigraphic Control and Chronology of the Sedimentation

The rich fossil content of the samples allows locate accurately the main biostratigraphic events relative to the planktonic foraminifera [11] and the calcareous nannoplankton [37]. However, no paleomagnetic data are successfully available at ODP-site 975 due to that strong magnetic overprinting obliterated the primary magnetization [10]. Regarding the planktonic foraminifera, the most significant Pliocene–Gelasian events in the Mediterranean realm identified in the ODP-site 975 (Figure 6) allow the bio-chronostratigraphic monitoring. The chronometry of the events is based on the age estimates by ATNTS 2004 [38] for the Eastern Mediterranean from data by [39–44].

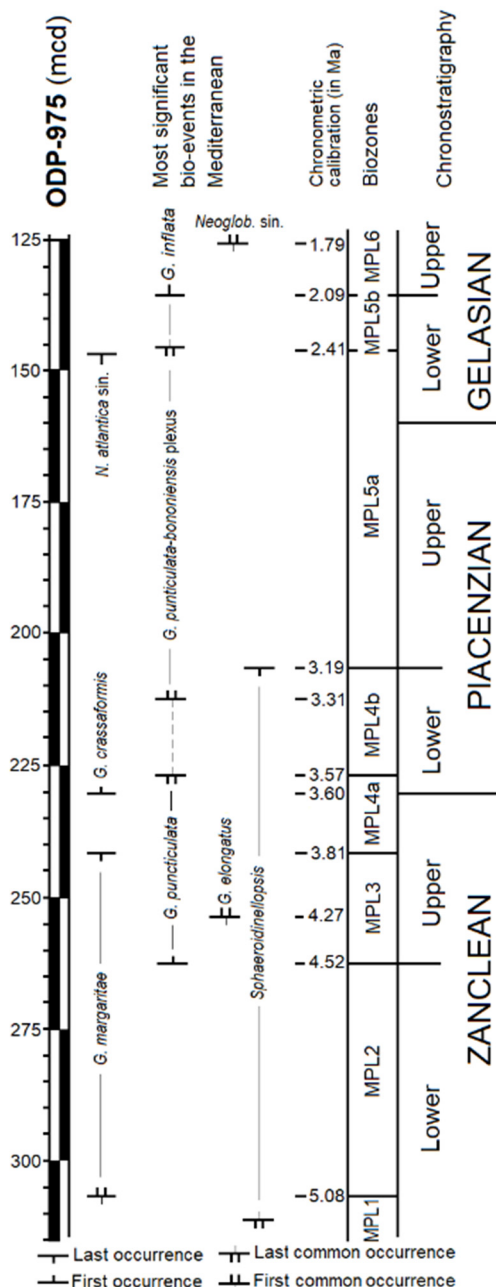


**Figure 6.** Chronologic monitoring of the Pliocene–Gelasian sedimentation at ODP-site 975 based on planktonic foraminifera. Biozones by [45], amended by [46].

The base of the Pliocene marine deposition (Unit I by [10]) in the Site-975 locates at 314.8 mcd (meters composite depth). Above, the first analyzed level (311.6 mcd) contains frequent *Sphaeroidinellopsis*

(3% in the planktonic foraminifer assemblage; Figure 2) and few left-coiling *Neoglobobulimina*, characterizing the MPL1 zone by [45]. Specimens of *G. margaritae* are very rare up to the level 306.6 mcd, where it reaches the 7% of the assemblage. The first common occurrence (FCO) of this species (5.08 Ma) marks the beginning the MPI-2.

The first occurrence (FO) of *G. puncticulata* (4.52 Ma) clearly occurs at 262.2 mcd, where the species burst with high frequency (more than 25% in the assemblage). This datum defining the base of the MPL3 is frequently used as a marker for the Lower/Upper Zanclean boundary [45,47–49]. Above, from the 253.3 mcd is observed a sharp increase in the frequency of *G. ruber*–*G. elongatus*, coexisting with abundant specimens of *G. extremus* in a continuous range of morphologic variability among them. Although the *G. elongatus* type appears rarely in Mediterranean sections from the Upper Messinian [50], this sudden irruption with high frequencies during the late Zanclean seems have a remarkable biostratigraphic interest. Based on the sedimentary rates, the FCO of *G. ruber*–*G. elongatus* occurred close to 4.27 Ma. The following significant event referred to the last occurrence (LO) of *G. margaritae* (3.81 Ma) was noticed at 241.4 mcd. This bioevent marks the base of the MPL4a zone in the uppermost Zanclean.

The magnetic shift Gilbert/Gauss (3.60 Ma) has been proposed as a global marker for the correlation of the Zanclean/Piacenzian boundary [51]. In the proximity of this limit, the authors noticed the occurrence of two planktonic foraminiferal events: the FO of *G. crassaformis* (3.60 Ma) and the temporal disappearance *G. puncticulata* beginning in 3.57 Ma; (*G. crassaformis* shows an ample morphologic spectrum ranging from rounded forms to keeled ones, and as a result, the location of the first occurrence is inaccurate. In the sediments drilled at the ODP-site 975, we noted that from the level 229.6 mcd the sediments yield morphotypes assignable to *G. crassaformis* with scarce specimens showing an imperforate peripheral band. However, as low as from the level 236.9 mcd appear specimens morphologically close to *G. crassaformis* showing spiral side almost flat and a sharp periphery. These specimens seem to have derived from typical *G. puncticulata*, as they are linked by intermediate forms. Anyway, the location of the FO of *G. crassaformis* in the Site 975 at the level 229.6 mcd carries imprecision. A most suitable event is the temporal (quasi-) disappearance of *G. puncticulata* which is clearly perceptible in the interval between 226.61 and 211.91 mcd, where only very occasionally some specimen of this species appears. The onset of this temporal disappearance of *G. puncticulata* was used by [45] for marking the base of MPL4b zone. When *G. puncticulata* reappears (3.31 Ma) above 212 mcd, the populations show frequent morphotypes attributable to *G. bononiensis*. The last occurrence of *Sphaeroidinellopsis* ssp. located at 205.91 mcd (3.19 Ma) allows to characterize the beginning of the Late Piacenzian sedimentation.

The Gelasian was introduced by [52] as a new stage for covering the last part of the Pliocene. However, based on that this stage is characterized by the occurrence of major glacial cycles in the northern hemisphere, it was incorporated to the Pleistocene series [53]. The base of the Gelasian, dated in 2.588 Ma (isotopic stage 103; [38]), coincides practically with the Gauss/Matuyama magnetic reversal and thus this paleomagnetic shift is an excellent tool for the global correlation. In terms of planktonic foraminifera, two significant events have been pointed out close to the beginning of the Gelasian [54]: (i) a short time-span characterized by the presence of the *N. atlantica* (sin) topped in 2.41 Ma and (ii) the L(C)O of *G. bononiensis* dated at 2.41 Ma also.

In the interval including the samples from 144.79 mcd to 145.23 mcd is noted the presence of frequent left-coiling *N. atlantica* representing between 2%–5% of the planktonic foraminifer assemblages, whereas in upper samples this form was absent. Moreover, the last sample before the 2nd disappearance of the *G. puncticulata*–*G. bononiensis* plexus is 143.79 mcd. Based on the observed homogenous sedimentation, it can be considered a constant sedimentary rate near to the critical time-span of the Piacenzian/Gelasian transition. In this suppose, the onset of the Gelasian deposition must be located between the levels 158.3 and 159.3 mcd.

The most significant foraminifer event through the Gelasian times is the FO of *G. inflata* (2.09 Ma). The reappearance of the *G. puncticulata*–*G. bononiensis*–*G. inflata* plexus (made up predominantly

by *G. inflata* morphotypes) occurs abruptly, reaching for almost half of components of the planktonic assemblage (45% in the level 134.34 mcd). Thus, this event allows an easy chronostratigraphic partition of the Gelasian.

The top of the chronostratigraphic interval analyzed was the Gelasian/Calabrian boundary, astronomically tuned in 1.806 Ma [38]. Specifically, for Mediterranean sections, the FCO of left-coiling specimens of *Neogloboquadrina* can be used as a proxy bio-event for the onset of the Calabrian open-sea sedimentation [36]. In the Site-975 section, the level 125.4 mcd (dated in 1.79 Ma) yields left-coiling *Neogloboquadrina* by more than 10% of the planktonic foraminifer assemblage. However, it must be emphasized that in the >150  $\mu\text{m}$  fraction the typical *N. pachyderma* are rare, whereas the most of specimens respond to intermediate *N. dutertrei*–*N. pachyderma* (left coiling) morphologies and, probably, the environmental requirements of these forms differ of those of the present *N. pachyderma*.

## 5. Results

The general curves corresponding to the analyzed sea-surface parameters: temperature, seasonality and salinity, show an expectable variation of values through the Pliocene and Gelasian (Figure 7). For easing the comments and discussion on the results, references relative to the present-day values of the sea surface in the Balearic area are included: 18.7 °C for the average annual SST; 13.8 °C for the winter-SST; 23.6 °C for the summer-SST; 9.8 °C for the seasonality; and 37.3‰ for the salinity. In addition, considering the high values of seasonality and salinity in the area, as standard references are included the average seasonality value obtained from the sites of the calibration database (6.0 °C) and 35.0‰ as the sea mean salinity. Finally, also were selected the value 38‰ as a reference of high salinity featuring the sea surface of the Eastern Mediterranean.

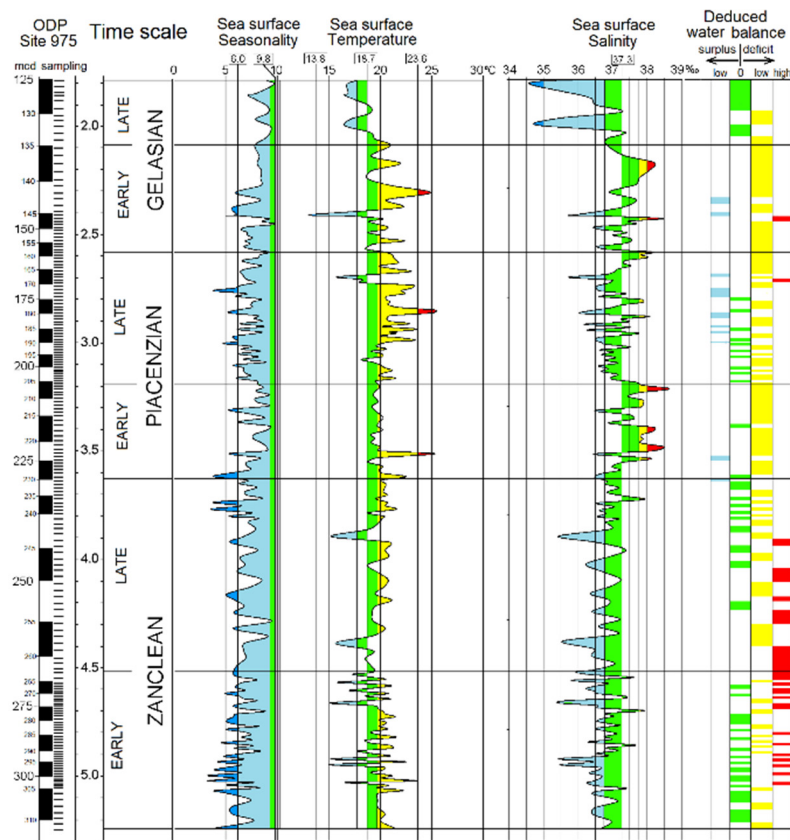


**Figure 7.** Variations of the paleoceanographic parameters and water balance through Pliocene–Gelasian.

The results for the complete dataset of the Pliocene–Gelasian sampling provide a mean value of  $19.9 \pm 1.9$  °C for the SST (Table 3), which is slightly higher (+1.2 °C) than the present SST in the

area, but within of the range of the standard deviation ( $\sigma$ ). Nevertheless, taking in account that the mean seasonality was  $7.0 \pm 1.4$  °C, up to 2.8 °C lower than the present-day value, it can deduce that, in whole, the Pliocene–Gelasian waters were significantly warmer during the winters (about +3 °C), whereas temperatures were similar during the summers. Regarding the salinity, the mean value ( $36.9\text{‰} \pm 0.7\text{‰}$ ) is near 2‰ higher in comparison with the standard reference, but it is slightly below ( $-0.4\text{‰}$ ) than that of the present-day in the area, showing that the high salinity of the Mediterranean also was a feature of the Balears area during the Pliocene–Gelasian times. Nevertheless, the general curves show significant thermo-salinity differences through the Pliocene and Gelasian (Figure 7, Table 3).

**Table 3.** Mean values of the oceanographic parameters for the different time intervals.

TIME INTERVAL	SST $\pm \sigma$ (°C)	SST-Winter $\pm \sigma$ (°C)	SST-Summer $\pm \sigma$ (°C)	Seasonality $\pm \sigma$ (°C)	Salinity $\pm \sigma$ (‰)
Present-day Balears	18.7	13.8	23.6	9.8	37.3
Gelasian–Pliocene	19.9 $\pm$ 1.9	16.4 $\pm$ 2.2	23.4 $\pm$ 1.8	7.0 $\pm$ 1.4	36.9 $\pm$ 0.7
Late Gelasian	18.1 $\pm$ 1.4	13.8 $\pm$ 2.4	22.4 $\pm$ 1.5	8.6 $\pm$ 0.8	36.1 $\pm$ 0.9
Early Gelasian	19.6 $\pm$ 2.5	15.8 $\pm$ 2.4	23.3 $\pm$ 2.7	7.5 $\pm$ 1.2	37.3 $\pm$ 0.7
Gelasian	19.2 $\pm$ 2.4	15.1 $\pm$ 2.3	23.0 $\pm$ 2.4	7.8 $\pm$ 1.2	36.9 $\pm$ 0.9
Late Piacenzian	20.9 $\pm$ 1.7	17.4 $\pm$ 2.0	24.4 $\pm$ 1.6	7.0 $\pm$ 1.1	37.0 $\pm$ 0.5
Early Piacenzian	20.0 $\pm$ 1.3	16.2 $\pm$ 1.8	23.9 $\pm$ 1.1	7.7 $\pm$ 1.4	37.6 $\pm$ 0.6
Piacenzian	20.6 $\pm$ 1.6	17 $\pm$ 2.0	24.2 $\pm$ 1.5	7.2 $\pm$ 1.3	37.2 $\pm$ 0.6
Late Zanclean	19.7 $\pm$ 1.3	16.3 $\pm$ 1.6	23.1 $\pm$ 1.3	6.8 $\pm$ 1.3	36.8 $\pm$ 0.5
Early Zanclean	19.7 $\pm$ 1.8	16.6 $\pm$ 2.2	22.8 $\pm$ 1.6	6.2 $\pm$ 1.4	36.7 $\pm$ 0.5
Zanclean	19.7 $\pm$ 1.7	16.5 $\pm$ 2.0	22.9 $\pm$ 1.5	6.4 $\pm$ 1.4	36.7 $\pm$ 0.5

In the Zanclean, the SST fluctuate around 19.7 °C, close to the average value obtained for the entire Pliocene–Gelasian interval, but with a lower seasonality (6.2–6.4 °C), suggesting that, as a whole, the summer-SST were slightly cooler and the winter-SST near 3 °C warmer in relation to the present-day values. During the Early Zanclean occurred phases of large thermic fluctuations, in where temperatures change for more than 5 °C between consecutive samples (i.e., between 5.1–4.9 Ma and between 4.7–4.5 Ma), whereas the SST fluctuations appear to decrease in the Late Zanclean, as reflected by a smaller dispersion ( $\sigma = 1.3$  °C vs.  $\sigma = 1.8$  °C). In the Zanclean, the salinity maintains predominantly values (36.7‰–36.8‰) below that of present-day in the area and only very occasionally, high-salinity peaks are noted. It is noteworthy that the levels of lower salinity (around 35.5‰) strictly coincide with those of lower SST close to 15 °C.

As in the Late Zanclean, during the Piacenzian the SST are maintained near permanently above the current value in the area, showing a clear tendency to increase through the interval. For the Early Piacenzian, the mean temperature estimated was of 20.0 °C, with a maximum peak exceeding 25 °C noticed in 223.61 mcd (3.51 Ma). The mean seasonality shows also a high relative value ( $7.7 \pm 1.4$  °C), although it is still most than 2 °C below to that of the present-day in the area. In any case, these estimations could indicate that the SST during the winter (around 16.2 °C) were similar to those of the Zanclean, while the summer-SST (around 23.9 °C) could be even slightly above the current value for this season in the area. However, the most noteworthy feature for the Early Piacenzian relates to the salinity, reaching the higher average value ( $37.6\text{‰} \pm 0.6\text{‰}$ ) of all studied intervals. This mean value is above the present-day salinity in the area and frequently reaches the current high salinity of the Eastern Mediterranean (38‰) and even it exceeds the 38.5‰ in several episodes.

In the Late Piacenzian, the mean SST increases up to 20.9 °C, providing the highest values in the entire studied time-span. Considering the mean seasonality (7.0 °C) with a relatively small dispersion of values ( $\sigma = 1.1$  °C), these results suggest very warm summer-SST around 24.4 °C, whereas the SST during the winters would fluctuate around 17.4 °C. It is clearly appreciable an increasing-decreasing cycle through the interval reaching a maximum temperature in a short episode located at 179–181 mcd (2.85–2.86 Ma), when temperatures exceed 25 °C. On the contrary, the upper part of the late Piacenzian show a decreasing tendency of the SST, including a short cold episode between 169.30–167.30 mcd (2.72–2.70 Ma) when the temperatures fallen up to a minimum peak of 15.8 °C. Regarding the salinity,

the estimates are clearly lower than the Early Piacenzian, offering an average value ( $37.0\text{‰} \pm 0.5\text{‰}$ ) that is slightly lower to that occurring currently in the Balearic area.

The SST estimates for the Gelasian show an average value of  $19.2\text{ °C}$ , thus indicating a drop in temperature of most than  $1.5\text{ °C}$  with respect to the Late Piacenzian. In addition, it is noteworthy the increase in the standard deviation up to  $2.4\text{ °C}$  that reflects large thermal changes during the interval. The greater changes of the SST are mainly located in the middle part of the early Gelasian, between  $146.21\text{--}140.79\text{ mcd}$  ( $2.43\text{--}2.27\text{ Ma}$ ). In this time-span occurs the lowest SST for the complete Pliocene–Gelasian period, that was estimated in  $13.1\text{ °C}$  at the level  $144.79\text{ mcd}$  ( $2.41\text{ Ma}$ ) and a maximum peak close to  $25\text{ °C}$  at  $141.79\text{ mcd}$  ( $2.31\text{ Ma}$ ). In addition, there is a maximum SST difference of up to  $+9\text{ °C}$  between consecutive levels ( $144.79\text{--}143.79\text{ mcd}$ ) close to  $2.40\text{ Ma}$ . The extreme values of temperatures correspond generally with low seasonalities around  $5\text{--}6\text{ °C}$ , but for the entire Gelasian the average value ( $7.8 \pm 1.2\text{ °C}$ ) is relatively high and specifically for the Late Gelasian reaches up to  $8.6 \pm 0.8\text{ °C}$ , which is near of the current seasonality in the area.

The first part of the Early Gelasian shows features similar to the Late Piacenzian, but the transition to the Late Gelasian is characterized by large paleoceanographic changes. These changes can be concreted by a significant decrease of the SST in combination with an increase of the seasonality and a strong fall of the salinity. The mean SST estimated for the Late Gelasian was  $18.1\text{ °C}$  with small fluctuations ( $\sigma = 1.4\text{ °C}$ ), thus indicating a drop of  $1.5\text{ °C}$  with respect to the Early Gelasian and near  $3\text{ °C}$  below from the late Piacenzian. This leads to that the late Gelasian is the only time-span studied with a mean SST lower ( $-0.6\text{ °C}$ ) than the current value in the Balearic area. The low temperatures were accompanied by high seasonality values around  $8.6\text{ °C}$  and a standard deviation ( $\sigma = 0.8\text{ °C}$ ) that almost embraces the present-day value, in such a way that, as a whole, the winters were similar to the today, whereas the summers were more than  $1\text{ °C}$  lower. On the contrary, the average salinity for this interval ( $36.1\text{‰} \pm 0.9\text{‰}$ ) is as much as  $1.2\text{‰}$  below the current value in the area, although it still represents more than  $1\text{‰}$  above the reference of normal oceanic salinity.

## 6. Discussion of the Results: Paleoceanographic Interpretation

The changes showing the general sequences of the oceanographic parameters throughout the Pliocene and Gelasian (Figure 7) must be related to astronomically forced climatic oscillations and, occasionally, to catastrophic events, which led to different paleoceanographic settings.

Nevertheless, in the Mediterranean semiconfined framework, the paleoceanographic changes can be enlarged according to the water balance. Thus, in periods of water high deficit, it may be expected that the surface water of the Western Mediterranean would be predominantly fed by the inflows of Atlantic water, establishing conditions similar to those of the Alboran Sea, with seasonality and salinity less pronounced than in the present-day Balearic area. The SST would vary depending on the overall cold/warm climate balance, which would be reflected in the SST of the Canary Current entering the Mediterranean Sea. In warm periods, similar conditions to current subtropical waters could be achieved, with SST-mean above  $21\text{ °C}$  and low seasonality.

Periods of low water deficit in the Mediterranean, smaller than today, could lead to that the most of the Atlantic surface water entering the Mediterranean, due to the Coriolis effect, would flow mainly near the North African coast towards the Central and Eastern Mediterranean, whereas the surface water current in the Western Mediterranean would be significantly fed by the return flow from the Levantine Basin. This framework suggests high salinity values and relatively low seasonality in the Balearic area, establishing conditions similar to those of the current Central-Eastern Mediterranean. The SST would be increased in relation to the general climate balance, due to the insolation during the long period of residence of the water in the interior of the Mediterranean.

On the contrary, during the water-surplus periods by continental water inputs, a well-defined water stratification would be established with a relatively low-salinity and low-seasonality surface layer flowing into the Atlantic.

In analyzing the results in a general way (Figure 7), it is noteworthy that while the SST and salinity estimations fluctuate around the present-day values in the Balearic area, the seasonality offers permanently lower estimates. Even during the time-spans in where the seasonality values are most frequently near the current value, these occur with different thermohaline conditions (Table 3). Thus, in the Early Piacenzian, the relative high average-seasonality ( $7.7 \pm 1.4$  °C) is accompanied by temperate-high average-SST ( $20.0 \pm 1.3$  °C) and very high salinity ( $37.6\text{‰} \pm 0.6\text{‰}$ ), while in the Late Gelasian, the high seasonality ( $8.6 \pm 0.8$  °C) is given with lower SST conditions ( $18.1 \pm 1.4$  °C) and a relative low salinity ( $36.1\text{‰} \pm 0.9\text{‰}$ ). Considering that the current high seasonality (9.8 °C) in the Balearic area is mainly induced by the action of the winter-cold northern winds (Mistral and Tramontana), in combination with the summer invasion of warm and very saline water from the Eastern Mediterranean, it seems to be inferred that this paleoceanographic framework was rare or less pronounced during the Pliocene–Gelasian.

In order to visualize the paleoceanographic interpretation for the different time-spans, the oceanographic parameters and geographical location of the modern analog closest to each sample of the Pliocene–Gelasian sequence were determined (Figure 8 and Supplementary Table S2).

### 6.1. Zanclean

The mean seasonality for the Zanclean ( $6.4 \pm 1.4$  °C) close to the present standard reference (mean for the calibration dataset) suggests that for most of this interval the seasonality in the Western Mediterranean was not significantly enhanced by the northern winter winds similar to those currently acting in the region. Considering that the average winter-SST was up to 2.5–3 °C higher than it is today, while the summer-SST is only 0.5–1 °C lower, it seems to indicate a small influence of the northern cold winds and, parallelly, the summer warm-water supply from the eastern Mediterranean was also slightly smaller.

The modern analogs of the Zanclean samples (Figure 8A and Supplementary Table S2) are distributed throughout a wide region spanning the Central and Western Mediterranean and the North Atlantic, from the Bay of Biscay to the Azores and Canary Islands (only the sample 267.0 mcd, dated in 4.58 Ma, finds its analog in the Western Atlantic, in the Gulf Stream waters). This distribution suggests that the paleoceanographic conditions in the Western Mediterranean during the Zanclean were predominantly influenced by a variable water deficit and, as a consequence, by the surface water mass of the Canary Current entering in the Mediterranean through the Strait of Gibraltar. In a general way, these results are in accordance with [55] suggesting that a Mediterranean-type climate, characterized by strong seasonality and a dry summer, may have existed in this region during the early Pliocene. Specifically, for the beginning of the Pliocene (5.5–5.0 Ma), [56] note a warmer and more humid climate than today, which seems to also reflect the results in the present study. However, the climate conditions vary throughout the Zanclean and a more detailed analysis it is necessary.

The scarce cold samples (9/85) below 17.7 °C, (SST-mean: 15.9 °C) have their analogs located very predominantly in the Bay of Biscay, corresponding to mean seasonality (6.7 °C) and salinity (35.7‰) near the average oceanographic values. These cold episodes can be consistent with dry stages in the Western Mediterranean, which would lead to a high water-deficit. In these conditions, the Canary Current with low temperatures could reach the Gulf of Cadiz invading the Western Mediterranean, thus also explaining the low values of salinity and seasonality in relation to those of the present-day.

A similar paleoceanographic interpretation, in a slightly less cold climate, can be applied to a set of samples that give estimates of temperate-SST with relatively low seasonality (4.6–6.5 °C) and salinity (36.3‰–36.6‰) and that locate their analogs in the Atlantic near Gulf of Cadiz and Alboran Sea (Figure 8A). The remain samples with temperate-SST estimates show mostly high seasonality (7.5–9.5 °C) and salinity (around 37‰) and most of their modern analogs are located in the Western Mediterranean, suggesting conditions close to that of the present-day in the Balearic area.

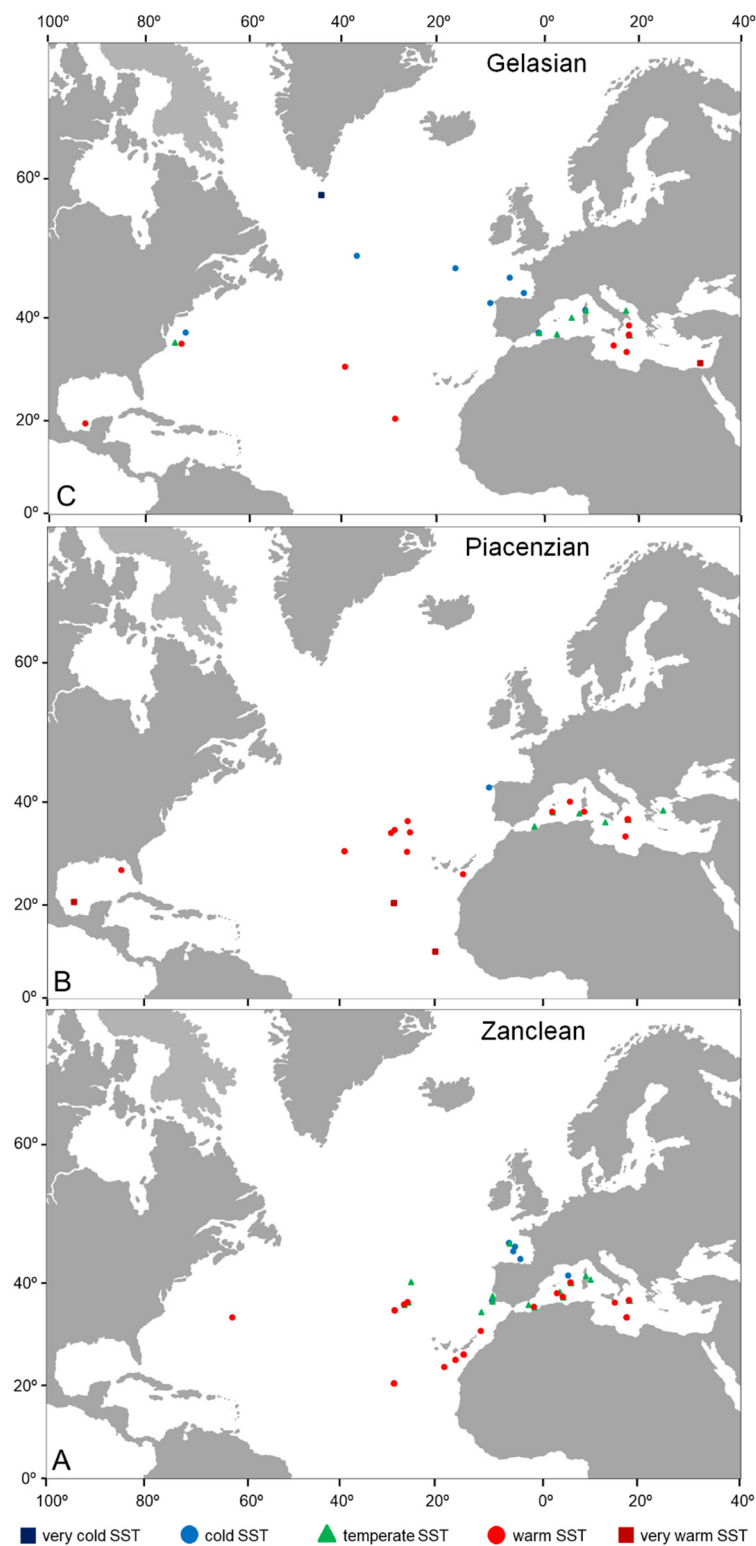


**Figure 8.** Location of the closest modern analogs to the Pliocene–Gelasian samples of the ODP-site 975. (A) Zanclean; (B) Piacenzian; (C) Gelasian.

The samples with warm-SST estimates ( $>19.7\text{ }^{\circ}\text{C}$ ; mean-SST =  $20.7\text{ }^{\circ}\text{C}$ ) predominate in the Zanclean. (50/85) and they find their modern analogs in the Mediterranean (mostly in the Central Mediterranean) and at low latitudes of the Atlantic (mainly in the Canary Islands area and tropical Atlantic). Samples having their analogs in the Mediterranean show high mean-values of seasonality

(7.5 °C) and salinity (37.2‰), approaching the current conditions, slightly warmer, in the Balearic area. On the other hand, samples with Atlantic analogs are characterized by showing low seasonality values (mean = 5.2 °C) and relative low salinity (mean = 36.7‰). These samples could represent warm episodes with low water deficit in the Mediterranean, allowing surface Atlantic water inputs and a very small return of surface water from the Levantine basin. Nevertheless, similar conditions could be reached during warm and humid episodes in the Mediterranean, resulting in a surplus water balance with surface outflow of warm and poor in salinity water from the Mediterranean towards the Atlantic.

### 6.2. Piacenzian

The main paleoceanographic features for this interval (Table 3) can be summarized in: (i) relatively high SST values, around  $20.6 \pm 1.6$  °C, with no estimates below the temperate-SST range; (ii) high seasonality, mainly during the early Piacenzian ( $7.7 \pm 1.4$  °C), which approximates the current one in the Balearic area; and (iii) high salinity waters, with an average value ( $37.2\text{‰} \pm 0.6\text{‰}$ ) similar to the current one, but there is episodes in which salinity reaches typical values of the Eastern Mediterranean ( $>38\text{‰}$ ).

Most Piacenzian samples reach warm or very warm SST values (57/74). Within this group, estimates more than 22 °C (12/57) are accompanied by relative low seasonality (5.7 °C) and salinity (36.5‰) values and the samples find their analogs (Figure 8B and Supplementary Table S2) mostly in the Canary Islands and tropical Atlantic area (two of them in the Gulf of Mexico). These values could be achieved in the Balearic area during warm and humid periods, in which the region could be mainly fed by eastern surface water with significant continental input and surface water outflow into the Atlantic. On the other hand, samples with warm and temperate SST values, between 22 and 18 °C (61/74), are accompanied by higher estimates of seasonality (7.5 °C) and salinity (37.4‰) and locate their closest modern analogs in the Mediterranean. It is noteworthy that 43 of these samples find the same analog located in the Central Mediterranean (37°12'N, 18°44'E). Together, these samples suggest oceanographic settings similar to the current one in the Western Mediterranean with slightly higher SST.

During the Early Piacenzian, the water deficit in the Mediterranean could be slightly higher than today, thus explaining the high salinity values. On the contrary, in the Late Piacenzian the climate in the Mediterranean region could be slightly warmer and humid, with alternation stages of low hydrological deficit and slight surplus, which could explain the fall in the salinity and seasonality values. [57] deduce that in the middle Pliocene (Late Piacenzian, ca. 3 Ma), the climate in the European and Mediterranean was warmer, wetter and less seasonal than in the present-day, with Mediterranean SST increasing between 2–4 °C, which is coherent with the results here obtained.

A latest Piacenzian sample (167.3 mcd) dated to 2.70 Ma represents the first cold episode (SST = 15.7 °C) pre-announcing the end of the Piacenzian warm period. This episode shows conditions similar to that of the current off coast Galicia area, in the NW Iberia and it is consistent with a wide consensus in that the first Pliocene significant cooling event in the Mediterranean region took place between 2.8 and 2.5 Ma [58].

### 6.3. Gelasian

The Gelasian paleoceanography in the Western Mediterranean is characterized by strong fluctuations in temperature and salinity (Figure 7). During the Early Gelasian, the SST estimates result predominantly higher than at the present in the Balearic area, except in a short interval (samples 144.79 and 145.20 mcd; 2.41–2.42 Ma) extremely cold, where the SST estimates result between 13–14 °C, which are the coldest of the whole studied time-span. The estimated age for this interval coincides with MIS 96 [59] corresponding to the main extension of continental ice sheets. [60–62] among others, point out that this episode could be favored by the establishment of large ice sheets in the northern hemisphere, as a consequence of the closure of the ocean gateways (e.g., Panamanian Gateway). The samples from this very cold episode find its current analogs in the Labrador Current waters at the southern

Greenland (Figure 8C and Supplementary Table S2). The expansion of large ice sheets could limit the circulation of the Gulf Stream to the anticyclonic turn of low latitudes, while the eastwards branch of the El Labrador Current could be the main source of the Canary Current, introducing very cold waters into the Mediterranean throughout the whole annual cycle and thus maintaining relatively low values of seasonality (5–6 °C) and salinity (around 36‰).

Subsequent to the very cold episode, a particularly warm interval occurs, in which the SST estimate reaches up to 24.9 °C at 141.79 mcd (2.31 Ma), thus reflecting the establishment of glacial-interglacial climatic oscillations initiated at that time-span [55,63–65]. This level of high SST and low seasonality (5.9 °C) finds its analog in the Eastern Mediterranean, near the Nile delta and is likely to respond to an episode of water surplus in the Mediterranean. Similar conditions could be given for level 143.79 mcd, dated to 2.38 Ma (SST-22.1 °C; seasonality-5.7 °C), that locates its modern analog in the tropical Atlantic.

The rest of the samples of the Early Gelasian offers SST estimates (20.1 °C), relatively high, which are accompanied by salinity fluctuating around the current value in the area and by seasonality values around 7.7 °C. Most of these samples find the same modern analog in the Central Mediterranean (Figure 8C and Supplementary Table S2), to the south of Italy (specifically at 18.73° E, 37°20' N), suggesting a paleoceanography framework similar to the current one of the Western Mediterranean, although generally with a lower influence of the winter cold waters of the Gulf of Lyon.

The paleoceanography of the Late Gelasian is characterized by a more generalized cooling accompanied by relatively high seasonality and low salinity values (Table 3). In particular, it is noteworthy the presence of two quite cold episodes with SST around 17 °C, corresponding to episodes of very low salinity, generally lower than 36‰ and seasonality around 8.3 °C. Most of the samples of these episodes find their current analogs in the Bay of Biscay (Figure 8C and Supplementary Table S2), suggesting that the Western Mediterranean would be subjected to a strong influence of cold Atlantic waters. However, the high seasonality would indicate that summer SST would reach between 20–21.6 °C, showing a summer warming in the interior of the Mediterranean, probably as a consequence of a poor water renewal. These conditions could be achieved with a small or quasi null water-deficit at the Mediterranean, which in turn would affect a slow circulation, favoring the stratification of the water with the surface layer of low salinity. It is striking that two of these samples find their current analogs off coast Eastern USA, in the area affected by the exchange of cold waters of the Labrador Current and the warm waters of the Gulf Stream.

The abovementioned cold episodes alternate with warmer intervals, showing mean-values of SST around 19 °C, seasonality around 9 °C and salinity around 37‰, suggesting a paleoceanographic frame very similar to the current one. In fact, the modern analogs of these samples are all located in the western Mediterranean, around the Balearic area (Figure 8C and Supplementary Table S2).

## 7. Conclusions

The modern analog technique applied to the assemblages of planktonic foraminifera yielded from the Pliocene and Gelasian sediments drilled in the ODP Site 975 (Balearic area) has allowed to characterize the paleoceanography of the surface waters of the Western Mediterranean. Estimates of temperature, seasonality and salinity were obtained from a metric sampling through the section.

A restriction of the available taxonomic variables is necessary in order to establishing analog assemblages in the current calibration dataset and in the Pliocene–Gelasian sampling. The small estimation errors involving these adaptations, evaluated on the calibration dataset itself, result no significant in order to establishing general paleoceanographic features and trends through the time-span studied.

Overall, the results show that the average SST was around one degree Celsius higher in the Zanclean than in the present-day in the same area, ascending to two degrees Celsius in the late Piacenzian, when the SST reached for more than 25 °C sometimes. The rise in temperature is noted specifically in the winter season (2.5–3.5 °C), while summer values were similar to the present-day.

The Gelasian is a cooling period that led to the average-SST about  $-0.5^{\circ}\text{C}$  compared to today. The lowest SST ( $13.1^{\circ}\text{C}$ ) is reached in the early Gelasian, towards 2.41 Ma BP, although the late Gelasian is overall the coldest interval.

Regarding seasonality estimates, during the Pliocene–Gelasian they are permanently lower than in the present-day, thus suggesting that the current conditions in the area were rare, particularly in that affecting to the influence of the northern cold winds in winter. Through Gelasian, there is an increase in seasonality that punctually reaches values above nine degrees Celsius, establishing a regimen more similar to the current one.

From the combination of the sea-surface temperature, seasonality, and salinity results is deduced that the current deficit water regime in the Mediterranean was clearly predominant through the Pliocene and Gelasian. However, since Piacenzian this regime alternates with stages of water surplus, which are especially frequent in the late Piacenzian. By the middle of the early Gelasian, the regimen becomes more clearly in deficit again.

**Supplementary Materials:** The following are available online at <http://www.mdpi.com/2076-3263/10/8/302/s1>, Table S1: Census of the taxa in the Pliocene-Gelasian sediments of the ODP-site 975, Table S2: Estimates parameters and location of the modern analogs.

**Funding:** This study was supported with funding provided by Research Group RNM-146 of the “Junta de Andalucía” and project CGL2016-78577-P of the Government of Spain.

**Acknowledgments:** I gratefully acknowledge constructive remarks and suggestions from two anonymous reviewers.

**Conflicts of Interest:** The author declares no conflict of interest. The funders had no role in the design of the study; in the collection, analyses, or interpretation of data; in the writing of the manuscript, or in the decision to publish the results.

## References

1. Lanoix, F. Project Alboran, étude hydrologique et dynamique de la Mer d' Alboran. *Rapp. Tech. OTAN* **1974**, *66*, 70.
2. Bethoux, J. Mean water fluxes across sections in the Mediterranean sea, evaluated on the basis of water and salt budgets and observed salinities. *Oceanol. Acta* **1980**, *3*, 79–88.
3. Baringer, M.O.; Price, J.F. A review of the physical oceanography of the Mediterranean Outflow. *Mar. Geol.* **1999**, *155*, 63–82. [[CrossRef](#)]
4. Hopkins, T.S. Physics of the Sea. In *Western Mediterranean*; Margalef, R., Ed.; Pergamon Press: Oxford, UK, 1985; pp. 100–125.
5. Millot, C. Circulation in the Western Mediterranean Sea. *J. Mar. Syst.* **1999**, *20*, 423–444. [[CrossRef](#)]
6. Rouchy, J.M.; Caruso, A. The Messinian salinity crisis in the Mediterranean basin: A reassessment of the data and an integrated scenario. *Sediment. Geol.* **2006**, *188–189*, 35–67. [[CrossRef](#)]
7. CIESM. The Messinian salinity crisis from mega-deposits to microbiology—A consensus report. In *CIESM Workshop Monographs*; Briand, F., Ed.; CIESM Publisher: Monaco City, Monaco, 2008; Volume 33, pp. 1–168.
8. Guerra-Merchán, A.; Serrano, F.; Garcés, M.; Gofas, S.; Esu, D.; Gliozzi, E.; Grossi, F. Messinian Lago-Mare deposits near the strait of Gibraltar (Malaga Basin, S Spain). *Palaeogeogr. Palaeoclimatol. Palaeoecol.* **2010**, *285*, 264–276. [[CrossRef](#)]
9. Serrano, F.; Guerra-Merchán, A. Comment on the paper “Lago Mare and the Messinian salinity crisis: Evidence from the Alboran Sea (S. Spain)” by Do Couto et al. *Mar. Pet. Geol.* **2015**, *65*, 334–339. [[CrossRef](#)]
10. Comas, M.C.; Zahn, R.; Klaus, A. *Proc. ODP, Init. Repts.*; Ocean Drilling Program 161; ODP: College Station, TX, USA, 1996. [[CrossRef](#)]
11. Serrano, F.; González Donoso, J.M.; Linares, D. Biostratigraphy and paleoceanography of the Pliocene at Sites 975 (Menorca Rise) and 976 (Alboran Sea) from a quantitative analysis of the assemblages of planktonic foraminifers. In *Ocean Drilling Program Leg 161, Scientific Results*; Comas, M.C., Zahn, R., Klaus, A., Eds.; ODP: College Station, TX, USA, 1999.
12. Hutson, W.H. The Agulhas Current during the Late Pleistocene, analysis of modern faunal analogs. *Science* **1980**, *207*, 64–66. [[CrossRef](#)]

13. Kucera, M.; Weinelt, M.; Kiefer, T.; Pflaumann, U.; Hayes, A.; Weinelt, M.; Chen, M.T.; Mix, A.C.; Barrows, T.; Cortijo, E.; et al. Reconstruction of sea-surface temperatures from assemblages of planktonic foraminifera: Multi-technique approach based on geographically constrained calibration datasets and its application to glacial Atlantic and Pacific Oceans. *Quat. Sci. Rev.* **2005**, *24*, 951–998. [[CrossRef](#)]
14. CLIMAP. Seasonal reconstruction of the Earth's surface at the last glacial maximum. *Geol. Soc. Am. Map Chart Ser.* **1981**, *36*, 1–18.
15. Kucera, M.; Weinelt, M.; Kiefer, T.; Pflaumann, U.; Hayes, A.; Weinelt, M.; Chen, M.T.; Mix, A.C.; Barrows, T.; Cortijo, E.; et al. Compilation of planktic Foraminifera census data, LGM from the Atlantic Ocean. *PANGAEA* **2005**. [[CrossRef](#)]
16. González Donoso, J.M.; Serrano, F.; Linares, D. Sea surface temperature during the Quaternary at ODP Sites 976 and 975 (western Mediterranean). *Palaeogeogr. Palaeoclimat. Palaeoecol.* **2000**, *162*, 17–44. [[CrossRef](#)]
17. Serrano, F.; González Donoso, J.M.; Palmqvist, P.; Guerra-Merchán, A.; Linares, D.; Pérez-Claros, J.A. Estimating Pliocene sea-surface temperatures in the Mediterranean: An approach based on the modern analogs technique. *Palaeogeogr. Palaeoclimat. Palaeoecol.* **2007**, *243*, 174–188. [[CrossRef](#)]
18. Serrano-Rebollo, F.; Serrano, F. *Palaeoceanographer*, a computer tool estimating paleoceanographic characteristics of the Quaternary and late Neogene sea surface Waters. *Geogaceta* **2008**, *44*, 219–222.
19. Thunell, R.C. Distribution of recent planktonic foraminifera in surface sediments of the Mediterranean Sea. *Mar. Micropaleontol.* **1978**, *3*, 147–173. [[CrossRef](#)]
20. Brunner, C.A. Distribution of planktonic foraminifera in surface sediments of the Gulf of Mexico. *Micropaleontology* **1979**, *25*, 325–335. [[CrossRef](#)]
21. Loubere, P. Oceanographic parameters reflected in the seabed distribution of planktonic foraminifera from the North Atlantic and Mediterranean Sea. *J. Foraminifer. Res.* **1981**, *11*, 137–158. [[CrossRef](#)]
22. Kallel, N.; Paterne, M.; Duplessy, J.C.; Verganud-Grazzini, C.; Pujol, C.; Labeyrie, L.; Arnold, M.; Fontugne, M.; Pierre, C. Enhanced rainfall in the Mediterranean region during the last sapropel event. *Oceanol. Acta* **1997**, *20*, 697–712.
23. Conkright, M.E.; Locarnini, R.A.; García, H.E.; O'Brien, T.D.; Boyer, T.P.; Stephens, C.; Antonov, J.I. *World Ocean Atlas 2001: Objective Analyses, Data Statistics, and Figures. CD-ROM Documentation*; National Oceanographic Data Center: Silver Spring, MD, USA, 2002.
24. Prell, W.L. *The Stability of Low Latitude Sea-Surface Temperatures: An Evaluation of the CLIMAP Reconstruction with Emphasis on the Positive SST Anomalies*; University of California Press: Berkely, CA, USA, 1985.
25. Pflaumann, U.; Duprat, J.; Pujol, C.; Labeyrie, L.D. SIMMAX: A modern analog technique to deduce Atlantic sea-surface temperatures from planktonic foraminifera in deep-sea sediments. *Paleoceanography* **1996**, *11*, 15–35. [[CrossRef](#)]
26. Dowsett, H.J.; Robinson, M.M. Application of the Modern Analog Technique (MAT) of Sea Surface Temperature Estimation to Middle Pliocene North Pacific Planktonic Foraminifer Assemblages. *Palaeontol. Electron.* **1997**, *1*, 1–22. Available online: [http://palaeo-electronica.org/1998\\_1/dowsett/issue1.htm](http://palaeo-electronica.org/1998_1/dowsett/issue1.htm) (accessed on 20 June 2000). [[CrossRef](#)]
27. Ortiz, J.D.; Mix, A.C. Comparison of Imbrie-Kipp transfer function and modern analog temperature estimates using sediment trap and core top foraminiferal faunas. *Paleoceanography* **1997**, *12*, 175–190. [[CrossRef](#)]
28. González-Donoso, J.M.; Linares, D. Evaluation of some numerical techniques for determining paleotemperatures from planktonic foraminiferal assemblages. *Rev. Esp. Paleontol.* **1998**, *13*, 107–129.
29. Imbrie, J.; Kipp, N.G. A new micropaleontological method for quantitative paleoclimatology. Application to a late Pleistocene Caribbean core. In *The Late Cenozoic Glacial Ages*; Turekian, K.K., Ed.; Yale Univ. Press: New Haven, CT, USA, 1971; pp. 71–131.
30. De Vargas, C.; Norris, R.; Zaninetti, L.; Gibb, S.W.; Pawlowski, J. Molecular evidence of cryptic speciation in planktonic foraminifers and their relation to oceanic provinces. *Proc. Natl. Acad. Sci. USA* **1999**, *96*, 2864–2868. [[CrossRef](#)] [[PubMed](#)]
31. Bauch, D.; Darling, K.; Simstich, J.; Bauch, H.A.; Erlenkeuser, H.; Kroon, D. Palaeoceanographic implications of genetic variation in living North Atlantic *N. pachyderma*. *Nature* **2003**, *424*, 299–302. [[CrossRef](#)]
32. Darling, K.F.; Kucera, M.; Pudsey, C.J.; Wade, C.M. Molecular evidence links cryptic diversification in polar planktonic protists to Quaternary climate dynamics. *Proc. Natl. Acad. Sci. USA* **2004**, *101*, 7657–7662. [[CrossRef](#)]
33. Darling, K.F.; Wade, C.M. The genetic diversity of planktic foraminifera and the global distribution of ribosomal RNA genotypes. *Mar. Micropaleontol.* **2008**, *67*, 216–238. [[CrossRef](#)]

34. Darling, K.F.; Kucera, M.; Kroon, D.; Wade, C.M. A resolution for the coiling direction paradox in *Neogloboquadrina pachyderma*. *Paleoceanography* **2006**, *21*, 2011. [[CrossRef](#)]
35. Kucera, M.; Kennett, J.P. Causes and consequences of a middle Pleistocene origin of the modern planktonic foraminifer *Neogloboquadrina pachyderma* sinistral. *Geology* **2002**, *30*, 539–542. [[CrossRef](#)]
36. Serrano, F.; Guerra-Merchán, A. Sea-surface temperature for left-coiling *Neogloboquadrina* populations inhabiting the westernmost Mediterranean in the middle Pleistocene and the Pleistocene-Pliocene transition. *Geobios* **2012**, *45*, 231–240. [[CrossRef](#)]
37. De Kaenel, E.; Siesser, W.; Murat, A. Pleistocene calcareous nannofossil biostratigraphy and the Western Mediterranean sapropels, Sites 974 to 977 and 979. In *Proceedings of the Ocean Drilling Program: Scientific Results 161*; ODP: College Station, TX, USA, 1999; pp. 159–183. [[CrossRef](#)]
38. Lourens, L.; Hilgen, F.; Shackleton, N.J.; Laskar, J.; Wilson, D. The Neogene Period. In *A Geologic Time Scale 2004*; Gradstein, F.M., Ogg, J.G., Smith, A., Eds.; Cambridge University Press: Cambridge, UK, 2004; pp. 409–440.
39. Zachariasse, W.J.; Zijderveld, J.D.A.; Langereis, C.G.; Hilgen, F.J.; Verhallen, P.J.J.M. Early late Pliocene biochronology and surface water temperature variations in the Mediterranean. *Mar. Micropaleontol.* **1989**, *14*, 339–355. [[CrossRef](#)]
40. Hilgen, F.J. Astronomical calibration of Gauss to Matuyama sapropels in the Mediterranean and implication for the geomagnetic polarity timescale. *Earth Planet. Sci. Lett.* **1991**, *104*, 226–244. [[CrossRef](#)]
41. Hilgen, F.J. Extension of the astronomically calibrated (polarity) time scale to the Miocene/Pliocene boundary. *Earth Planet. Sci. Lett.* **1991**, *107*, 349–368. [[CrossRef](#)]
42. Langereis, C.G.; Hilgen, F.J. The Rossello composite: A Mediterranean and global reference section for the early to early late Pliocene. *Earth Planet. Sci. Lett.* **1991**, *104*, 221–225. [[CrossRef](#)]
43. Zijderveld, J.D.A.; Hilgen, F.J.; Langereis, C.G.; Verhallen, P.J.J.M.; Zachariasse, W.J. Integrated magnetostratigraphy and biostratigraphy of the upper Pliocene-lower Pleistocene from the Monte Singa and Crotona areas in Calabria, Italy. *Earth Planet. Sci. Lett.* **1991**, *107*, 697–714. [[CrossRef](#)]
44. Lourens, L.J.; Antonarakou, A.; Hilgen, F.J.; van Hoof, A.A.M.; Vergnaud-Grazzini, C.; Zachariasse, W.J. Evaluation of Plio-Pleistocene astronomical time scale. *Paleoceanography* **1996**, *11*, 391–413. [[CrossRef](#)]
45. Cita, M.B. Studi sul Pliocene e sugli strati di passaggio dal Miocene al Pliocene. VIII. Planktonic foraminiferal biozonation of the Mediterranean Pliocene deep sea record. A revision. *Riv. Ital. Paleontol. Stratigr.* **1975**, *81*, 527–544.
46. Sprovieri, R. Mediterranean Pliocene biochronology: A high resolution record based on quantitative planktonic foraminifera distribution. *Riv. Ital. Paleontol. Stratigr.* **1992**, *98*, 61–100. [[CrossRef](#)]
47. Zachariasse, W.J. Planktonic foraminiferal biostratigraphy of the Late Neogene of Crete (Greece). *Utrecht Micropaleontol. Bull.* **1975**, *11*, 1–171.
48. Borsetti, A.M.; Cati, F.; Colalongo, M.L.; Sartoni, S. Biostratigraphy and absolute ages of the Italian Neogene. *Ann. Geol. Hellen. 7th Internat. Congr. Medil. Neogene Athens* **1979**, *1*, 183–197.
49. Iaccarino, S. Mediterranean Miocene and Pliocene planktic foraminifera. In *Plankton Stratigraphy*; Bolli, H.M., Saunders, J.B., Perch-Nielsen, K., Eds.; Cambridge Univ. Press: Cambridge, UK, 1985; pp. 283–314.
50. Serrano, F. Los Foraminíferos Planctónicos del Mioceno Superior de la Cuenca de Ronda y su Comparación con los de Otras Áreas de las Cordilleras Béticas. Ph.D. Thesis, Publ. Univ. de Málaga, Málaga, Spain, 1979; p. 272.
51. Castradori, D.; Rio, D.; Hilgen, F.; Lourens, L. The Global Standard Stratotype-section and Point (GSSP) of the Piacenzian Stage (Middle Pliocene). *Episodes* **1998**, *21*, 1–6. [[CrossRef](#)]
52. Rio, D.; Sprovieri, R.; di Stefano, E. The Gelasian Stage: A proposal of a new Chronostratigraphic Unit of the Pliocene Series. *Riv. Ital. Paleontol. Stratigr.* **1994**, *100*, 103–124.
53. Gibbard, P.L.; Head, M.J.; Walker, M.J.C. Formal ratification of the Quaternary System/Period and the Pleistocene Series/Epoch with a base at 2.58 Ma. *J. Quat. Sci.* **2010**, *25*, 96–102. [[CrossRef](#)]
54. Gradstein, F.M.; Ogg, J.G.; Smith, A.G. *A Geologic Time Scale 2004*; Cambridge University Press: Cambridge, UK, 2004.
55. Bertoldi, R.; Rio, D.; Thunell, R. Pliocene-Pleistocene vegetational and climatic evolution of the south-central Mediterranean. *Palaeogeogr. Paleoclim. Palaeocl.* **1989**, *72*, 263–275. [[CrossRef](#)]

56. Fauquette, S.; Suc, J.-P.; Guiot, J.; Diniz, F.; Feddi, N.; Zheng, Z.; Bessais, E.; Drivaliari, A. Climate and biomes in the West Mediterranean area during the Pliocene. *Palaeogeogr. Paleoclim. Palaeocl.* **1999**, *152*, 15–36. [[CrossRef](#)]
57. Haywood, A.M.; Sellwood, B.W.; Valdes, P.J. Regional warming: Pliocene (3 Ma) paleoclimate of Europe and the Mediterranean. *Geology* **2000**, *28*, 1063–1066. [[CrossRef](#)]
58. Roveri, M.; Taviani, M. Calcarene and sapropel deposition in the Mediterranean Pliocene: Shallow- and deep-water record of astronomically driven climatic events. *Terra Nova* **2003**, *15*, 279–286. [[CrossRef](#)]
59. Lourens, L.J.; Becker, J.; Bintanja, R.; Hilgen, F.J.; Tuenter, E.; van de Wal, R.S.W.; Ziegler, M. Linear and non-linear response of late Neogene glacial cycles to obliquity forcing and implications for the Milankovitch theory. *Quat. Sci. Rev.* **2010**, *29*, 352–365. [[CrossRef](#)]
60. Mudelsee, M.; Raymo, M.E. Slow dynamics of the Northern Hemisphere glaciation. *Paleoceanography* **2005**, *20*, PA4022. [[CrossRef](#)]
61. Sarnthein, M.; Bartoli, G.; Prange, M.; Schmittner, A.; Schneider, B.; Weinelt, M.; Andersen, N.; Garbe-Schönberg, C.D. Mid-Pliocene shifts in ocean overturning circulation and the onset of Quaternary-style climates. *Clim. Past* **2009**, *5*, 269–283. [[CrossRef](#)]
62. Groeneveld, J.; Hathorne, E.C.; Steinke, S.; DeBey, H.; Mackensen, A.; Tiedemann, R. Glacial induced closure of the Panamanian Gateway during Marine Isotope Stages (MIS) 95–100 (~2.5Ma). *Earth Planet. Sci. Lett.* **2014**, *404*, 296–306. [[CrossRef](#)]
63. Backman, J. Pliocene biostratigraphy of DSDP Sites 111 and 116 from the North Atlantic Ocean and age of Northern hemisphere glaciation. *Stockh. Contrib. Geol.* **1979**, *33*, 115–137.
64. Thunell, R.C.; Williams, D.F. The step-wise development of Pliocene-Pleistocene paleoclimate and paleoceanographic conditions in the Mediterranean: Oxygen isotope studies and DSDP Site 125 and 132. *Utrecht Micropaleontol. Bull.* **1983**, *30*, 11–127.
65. Shackleton, N.; Backman, J.; Zimmerman, H.; Kent, D.; Hall, M.; Roberts, D.; Schnitker, D.; Baldauf, J.; Desprairies, A.; Homrighausen, R.; et al. Oxygen isotope calibration of the onset of ice-rafting and history of glaciation in the North Atlantic region. *Nature* **1984**, *30*, 620–623. [[CrossRef](#)]



© 2020 by the author. Licensee MDPI, Basel, Switzerland. This article is an open access article distributed under the terms and conditions of the Creative Commons Attribution (CC BY) license (<http://creativecommons.org/licenses/by/4.0/>).